CrossMark

Growth and characterization of cyclohexylaminium hydrogen phthalate hemihydrate nonlinear optical single crystals

R. Gomathi[1] · S. Madeswaran[1] · D. Rajan Babu[1]

Abstract Organic bulk single crystal of cyclohexylaminium hydrogen phthalate hemihydrate (CYHPH) was grown by slow cooling method using methanol as a solvent. The grown crystal belongs to orthorhombic system with *Pbcn* space group and it has various functional groups such as NH_3^+, phthalate and a water molecule. The cut off wavelength of CYHPH was found at 307 nm. Thermal analysis affirmed that the CYHPH compound was stable up to 146 °C and completely decomposed at 263 °C. The activation energy at 100 Hz, 1 and 10 KHz was found to be 0.31, 0.141 and 0.142 eV respectively. The grown CYHPH crystal exhibits third order nonlinear optical behavior.

1 Introduction

Primary amines are strong bases which can easily make bonds with carboxylic acid groups such as, succinic acid, phthalic acid, para-methoxybenzoic acid, phosphoenolpyruvic acid, 4-carboxybenzeneboronic acid [1–5] etc. Recently many phthalate groups have been found to exhibit ferroelectricity, piezoelectricity and nonlinear optical (NLO) properties [6–8]. Organic nonlinear optical crystals have garnered much attention due to their potential applications in second order, third order harmonic generation and electro-optic modulators [9, 10]. When compared to inorganic NLO materials, organic NLO materials have a higher nonlinear coefficient, inherent synthetic flexibility, easier fabrication, high resistance to optical damage and quick optical response time [11, 12]. Further the physical properties not only depend on the molecular structure but also have an influence on the supramolecular structure of the crystal. Supramolecular assembly of carboxylic acids is very important because they form hydrogen bond on their own and many other compounds [13–15]. In the field of crystal engineering, some of noncovalent interactions have been extensively used such as hydrogen bonding, coordination interaction, halogen bonding, π–π interaction and van der Waals weak interactions. These are the fundamental forces for molecular recognition ability through intermolecular interaction to form the supramolecular assembly, which leads to the crystal structure. Hydrogen bond played a major role in preparing the organic crystal and some hydrogen bonds are stronger than the weakest covalent bonds [16]. Hydrogen bonding predominates in crystal engineering strategies due to their high strength and directionality. Strong hydrogen bonds in particular like, O–H⋯O, O–H⋯N and N–H⋯O interactions create one, two and three dimensional networks in the crystals [17–19]. One dimensional organic single crystal was most appealing due to the light weight, compact size, easy fabrication, highly ordered molecule packing, eliminated grain boundaries, long range carrier diffusion and minimized defects which offer substantial potential for constructing high efficient photonic, electronic and optoelectronic systems [20]. Organic materials which have high π–electron delocalization with large third order nonlinear susceptibilities can be used for applications in optical switching [21]. Growth of single crystals has great attention in the field of electronic industry, photonic industry and fiber optic communication due to the absence of grain boundaries, anisotropy and the uniformity of the composition. The single crystals and their characterization towards

✉ S. Madeswaran
madeswaran.s@vit.ac.in

1 Department of Physics, School of Advanced Sciences, Advanced Materials Research Centre, VIT University, Vellore, India

device fabrication are important for both academic as well as applied research. Among the various methods, the slow evaporation technique occupies a prominent place due to its versatility and simplicity which yields good quality single crystals. The cyclohexylaminium hydrogen phthalate hemihydrate (CYHPH) crystal structure was solved by Jagan and Sivakumar et al. [22] and they form one dimensional supramolecular network. In this present paper we have grown a cyclohexylaminium hydrogen phthalate hemihydrate single crystal using slow evaporation technique. The grown crystals were characterized by FT-IR analysis, UV-Vis-NIR spectrum, thermo gravimetric and differential scanning calorimetry analysis (TG-DSC), dielectric constant and nonlinear optical studies. The formula of the title compound is $C_6H_{14}N^+ \bullet C_8H_5O_4^- \bullet 0.5H_2O$.

2 Experiments

2.1 Synthesis and bulk growth

The cyclohexylaminium hydrogen phthalate hemi hydrate single crystal (CYHPH) was synthesized by slow evaporation technique. Stoichiometric ratio (1:1) of cyclohexylamine (5.7 mL, 50 mmol) and phthalic acid (8.3065 g, 50 mmol) purchased from Sigma–Aldrich was dissolved in 50 mL of methanol. The mixed solution was stirred well for 4 h continuously to attain a homogeneous solution. Then the solution was filtered and kept undisturbed. The seed crystals were obtained from the mother solution after a period of 3 days. The purity of the crystal was improved by the recrystallization using methanol (Fig. 1a). The reaction scheme for the synthesis of CYHPH is as follows.
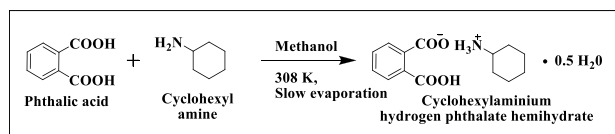
The growth kinetics of the crystal depends on the solubility and the temperature. Solubility of CYHPH was determined by gravimetrical method using methanol at different temperatures ranging from 30 to 50 °C (Fig. 2a). Initially the capacity of the 200 mL beaker with 100 mL of methanol was kept in a constant temperature bath having accuracy of 0.01 °C and CYHPH salt was added into the solvent at 30 °C and stirred using motorized stirrer to attain saturation. This procedure was repeated for the remaining temperatures (35–50 °C). From the solubility data it was observed that the material had a positive temperature coefficient. The solution was then cooled slowly to grow a bulk crystal of CYHPH. Based on the solubility data, 18.054 g of salt was dissolved in 150 mL of methanol solvent for the bath temperature at 40 °C and the saturated solution was stirred for 4 h continuously. The suitable tiny crystal (seed crystal) obtained from slow evaporation technique was used to grow a bulk crystal of CYHPH. The seed crystal was tied with a nylon thread and it was placed in the saturated solution. The temperature was gradually reduced at the rate of 0.1 °C per day. The colorless crystal with dimension up to $19 \times 15 \times 10$ mm^3 was harvested in a period of 20 days (Fig. 1b).

2.2 Characterization studies

Cyclohexylaminium hydrogen phthalate hemihydrate crystal was subjected to single crystal XRD analysis using

Fig. 1 **a** As grown CYHPH crystal from slow evaporation. **b** Bulk single crystal of CYHPH
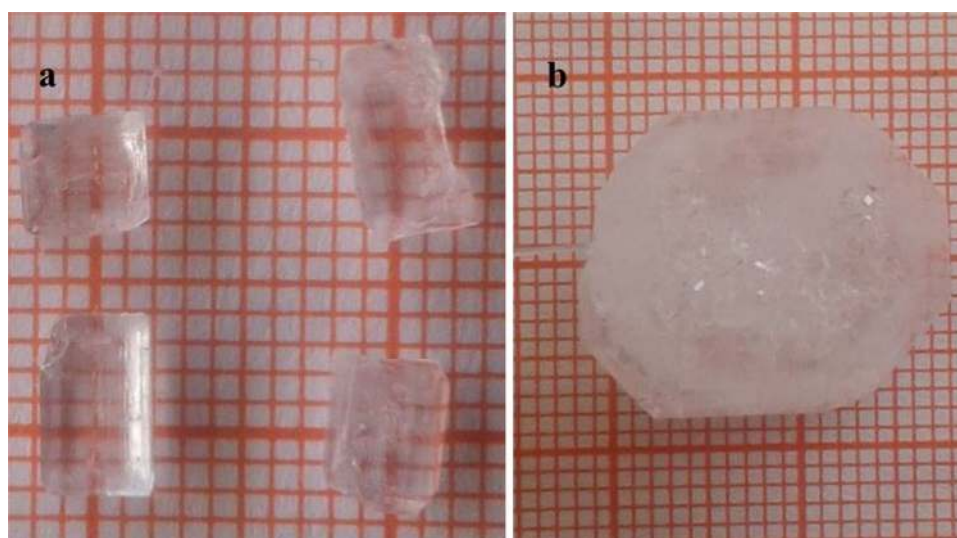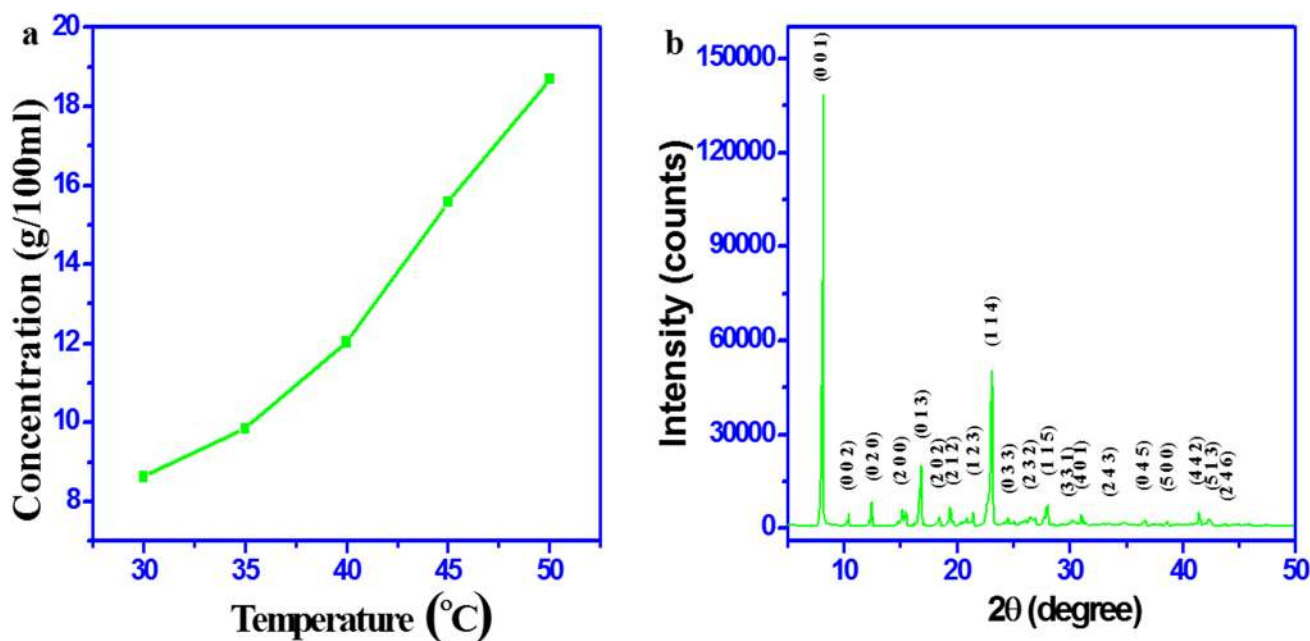
Fig. 2 **a** Solubility curve of CYHPH. **b** Powder XRD spectrum of CYHPH

Enraf Norius CAD4 diffractometer with MoKα radiation ($\lambda = 0.71073$ Å) to identify the cell parameters. A fine powder sample of CYHPH was also analyzed using BRUKER X-ray diffractometer with CuKα (1.5406 Å) radiation at the scan rate of 0.02 s^{-1}. The diffraction peak (h, k, l) values were indexed using powder-X software package. The FT-IR spectrum was employed in the range of 400–4000 cm^{-1} using SHMADZU IR Affinity-1s spectrometer with KBr pellet technique to confirm the presence of functional groups. Thermal analysis [TGA and DSC] were measured using SDT Q600 V20.9 Build 20 instrument in a nitrogen atmosphere with a heating rate of 20 °C min^{-1} from 30 to 600 °C. Optical absorption studies were carried out using Jasco-V-670 spectrometer in the range of 200–700 nm. The dielectric study was carried out as a function of frequency (100 Hz–5 MHz) using a Numetric Q impedance analyzer. Nonlinear optical properties were studied by Z-scan technique using He–Ne laser of wavelength 632.8 nm.

3 Results and discussion

3.1 X-ray diffraction analysis

The grown single crystal was subjected to an XRD analysis at 293 K. The cell parameters of CYHPH were calculated and it was found to belong to centro-symmetric *Pbcn* space group of orthorhombic system. The estimated cell parameters are agreed well with previous report [22] and presented in Table 1. The functional group decides

the crystal structure. Hydrogen phthalate anion with donor group was stabilized by delocalization of π electrons over the benzene ring. This delocalization enhances the nonlinear optical response in the material. As mentioned in the previous report by Jagan and Sivakumar et al. [22] cyclohexylaminium hydrogen phthalate hemi hydrate forms self-assembled supramolecular one dimensional network by the combination of N–H–O hydrogen bonds and C–H–O interactions. This hydrogen bonding induces the high molecular hyperpolarizability in the CYHPH crystal which ultimately enhances charge transfer properties and nonlinear optical absorption [23]. A powder sample of CYHPH was subjected to BRUKER X-ray diffractometer with CuKα (1.5406 Å) radiation and scanned from 5° to 60° at a scan rate of 0.02 s^{-1}. The diffraction peak (h, k, l) values were indexed using powder-X software package. The PXRD pattern is shown

Table 1 Cell parameters of CYHPH single crystal

Cell parameters	Calculated values	Reported values
a (Å)	11.662 (3)	11.6407 (2)
b (Å)	14.152 (5)	14.1463 (3)
c (Å)	16.932 (4)	16.9402 (4)
Alpha (degree)	90.00 (9)	90.00
Beta (degree)	90.00 (9)	90.00
Gamma (degree)	90.00 (0)	90.00
Volume (Å^3)	2794.8 (5)	2789.59 (10)
Space group	Orthorhombic (*Pbcn*)	Orthorhombic (*Pbcn*)
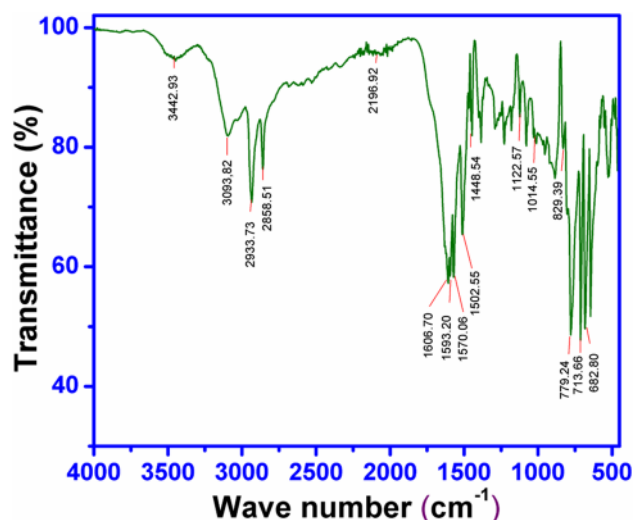
Fig. 3 FT-IR spectrum of CYHPH

Table 2 Assignment of vibrational frequency of CYHPH

Wave number (cm^{-1})	Assignments
3442.93	$-NH_3^+$ stretching
3093.82	$-OH$ stretching
2933.73, 2858.51	$-C-H$ stretching
2196.92	$-C\equiv N$ stretching
1606.70	$H-O-H$ stretching
1593.20	Asymmetry COO^- stretching
1570.06	$-N-H$ bending
1448.54	$-C-C$ stretching
1122.57	$-C-C-O$ stretching
1014.55	$-C-H$ in plan bending
779.24	$-NH_3^+$ rocking
713.66	$-C-C$ plane bending
682.80	$-COOH$ rocking

in Fig. 2b. The sharp peak appeared in PXRD spectrum which confirms the good crystalline nature of the grown crystal.

3.2 FT-IR analysis

The powder sample of CYHPH was analyzed using FT-IR analyzer with KBr pellet technique. The spectrum was recorded in the wave number range of 400–4000 cm^{-1} (Fig. 3). The presence of functional groups and their corresponding wavenumber are assigned in Table 2. There is a broad band nearly 3442 cm^{-1} representing the asymmetric stretching of NH_3^+ ion. The peak at 2858.5, 3093.82 and 2933.73 cm^{-1} represent the OH stretching and C–H stretching of CYHPH respectively [24]. Asymmetric stretching of

COO^- is presented in the range of 1593.20 cm^{-1}. Wavenumber at 1606.70 cm^{-1} confirms hydrogen bonding of water molecule [25]. Observation of above said functional groups confirms the formation of compound of CYHPH.

3.3 UV-Vis-NIR analysis

UV-Vis-NIR studies are essential to understand the electronic transition and to provide an idea about the band structure of the material. The UV-Vis-NIR absorption spectrum of CYHPH was taken in the range of 200–700 nm as shown in Fig. 4a. The cut off wavelength of the CYHPH compound is around 307 nm which is attributed to the transition of electron from non-bonding (n) orbital to anti-bonding π^* (n–π^*) due to the bonding of hydrogen phthalate anion with cyclohexylaminium cation. There was no other further absorption in the visible and near IR region (307–700 nm) which indicates that the crystal has a good transparency window resulting to suitable nonlinear optical applications. The optical absorption coefficient (α) was calculated using Tauc's relation [26].

$$(\alpha h v)^{1/n} = A(h v - E_g) \tag{1}$$

where, h is Plank's constant, E_g is energy gap, A is a constant, v is frequency of the incident photon and n is index (n = 1/2, 3/2, 2, 3) depends on the nature of electronic transition responsible for absorption.

Figure 4b shows the plot of hv versus αhv^2. Extrapolating of the linear portion of curve to the energy axis gives the value of the energy band gap (E_g). High value of E_g (4.08 eV) indicates very low defect concentration in the grown crystal which is typical of dielectric materials that possess inducing polarization when powerful radiation is incident on the material [27].

3.4 Thermal studies

Thermal analysis provides the information about the stability of the compound. Figure 5 shows the thermal behavior of the CYHPH crystal. Initially 6.3470 mg of CYHPH powder sample was taken for the analysis. The weight loss was occurred in three steps between 30 to 600 °C. The first weight loss (5.362%, 0.3403 mg) occurred from 70 to 170 °C, which specifies that the water molecule was present in the compound and the second step of weight loss (14.38%, 0.9128 mg) occurred from 190 to 210 °C which was due to the decomposition of ammonia [28, 29]. In third stage there was a major weight loss (80.25%, 5.093 mg) from 210 to 263 °C due to the decomposition of CO and CO_2 [30]. The DSC curve of CYHPH indicates that the
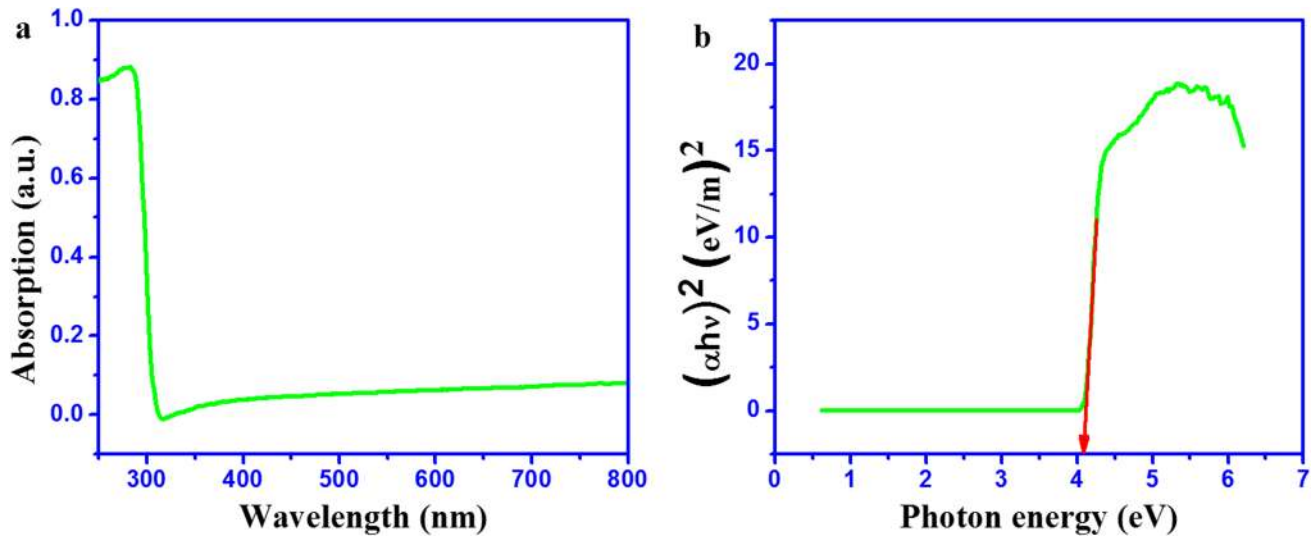
Fig. 4 **a** UV-Vis-NIR spectrum of CYHPH. **b** Tauc's plot of CYHPH
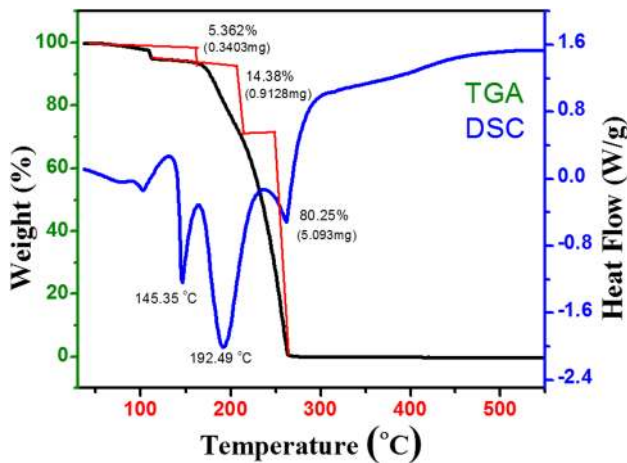
Fig. 5 TG-DSC studies of CYHPH

crystal had three sharp endothermic peaks at 103, 146 and 192 °C, confirming the presence of the water molecule, melting and decomposition points respectively. At 263 °C the crystal was completely decomposed. The melting point of the crystal was 146 °C, which was also confirmed by the melting point apparatus.

3.5 Dielectric studies

A study of the dielectric properties (dielectric constant and dielectric loss) of materials gives an understanding of the electrical field distribution within the material, various polarization mechanisms and structural transition. The dielectric studies of material are contributed by four types

of polarizations such as electronic, ionic, orientational and space charge polarization. These types of polarizations are more effective at low frequency range and decreased with increasing frequency. Opposite sides of suitable CYHPH crystal was coated with silver paste and inserted between the two nickel electrodes, resulting in the formation of a parallel plate capacitor. The dielectric constant and dielectric loss were measured as a function of frequency at various temperatures (30 to 100 °C) using the relation

$$\varepsilon_r = \frac{Cd}{\varepsilon_o A} \tag{2}$$

$$\text{Loss factor} = \frac{\varepsilon''}{\varepsilon'} \tag{3}$$

where ε_r is the dielectric constant of the material, ε_o the permittivity of free space ($8.854 \times 10^{-12} F/m$), A the area of the crystal, d the thickness of the sample, ε'' the imaginary part of the dielectric constant and ε' the real part of the dielectric constant. Figure 6a shows the dielectric constant of the sample versus applied frequency at different temperatures. The dielectric constant has maximum value in lower frequency region due to the presence of all types of polarizations. At higher frequency, the minimum value of the dielectric constant is attributed to the loss of substantial of these polarizations gradually [31]. Figure 6b shows the dielectric loss versus applied frequency over the temperature range of 30–100 °C. At high frequency, the minimum value of dielectric loss reveals that the crystal possesses enhanced optical quality with lesser defects.

From the dielectric data AC conductivity was also calculated using the relation,
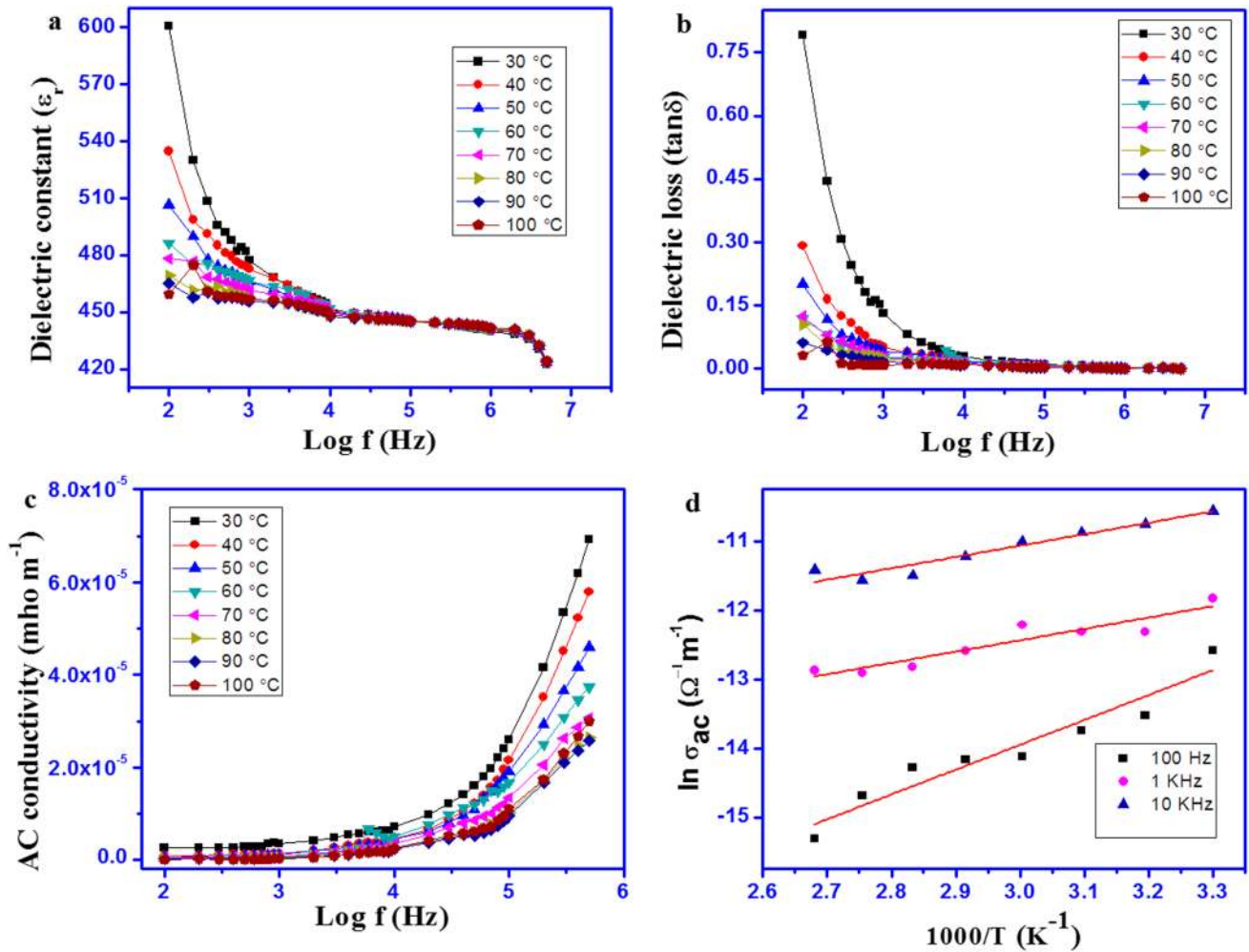
Fig. 6 a Dielectric constant as a function of frequency at different temperatures. **b** Dielectric loss as a function of frequency at different temperatures. **c** Ac conductivity at different temperatures. **d** Plot of 1000/T versus ln σ_{ac}

$$\sigma_{ac} = 2\pi f \varepsilon_0 \varepsilon_r \tan\delta$$

where, f frequency of the applied field and $tan\delta$ is dielectric loss of the crystal. Figure 6c shows the ac conductivity versus log frequency at different temperatures. AC conductivity depends on dielectric constant, loss factor and frequency. The conductivity increases with the increase in frequencies and decreases with temperature which is due to the reducing density of the crystal by thermal expansion [32]. The plot of $ln\sigma_{ac}$ versus 1000/T (shown in Fig. 6d) obeys the Arrhenius relationship $\sigma_{ac} = \sigma_0 \exp(\frac{-E_a}{KT})$, where K is the Boltzmann constant, E_a is the activation energy. The value of activation energy is at 100 Hz, 1 KHz and 10 KHz is 0.31, 0.141 and 0.142 eV respectively. The low value of activation energy indicates that less energy is required to take charge carriers in the conductivity process [33].

3.6 Z-scan technique

The Z-scan technique is a familiar technique used to determine both nonlinear refractive index and nonlinear absorption coefficient simultaneously by closed and open aperture respectively [34]. A He–Ne laser having a wavelength of 632.8 nm was used as an excitation source with the intensity of 5 mW. The sample of 0.56 mm thickness was scanned along the Z direction through a tightly focused beam which was filtered to attain Gaussian intensity profile. The focus of the polarized beam was passed through the converging lens of 30 mm focal length to offer the beam waist, ω_0=11.41 μm. Figure 7a and b show the closed and open aperture spectrum of the CYHPH crystal. In the closed aperture spectrum, the pre focal valley followed by pre focal peak evidences a positive sign of nonlinear refractive index, attributed to the self-focusing effect which is the result of non-uniform spatial
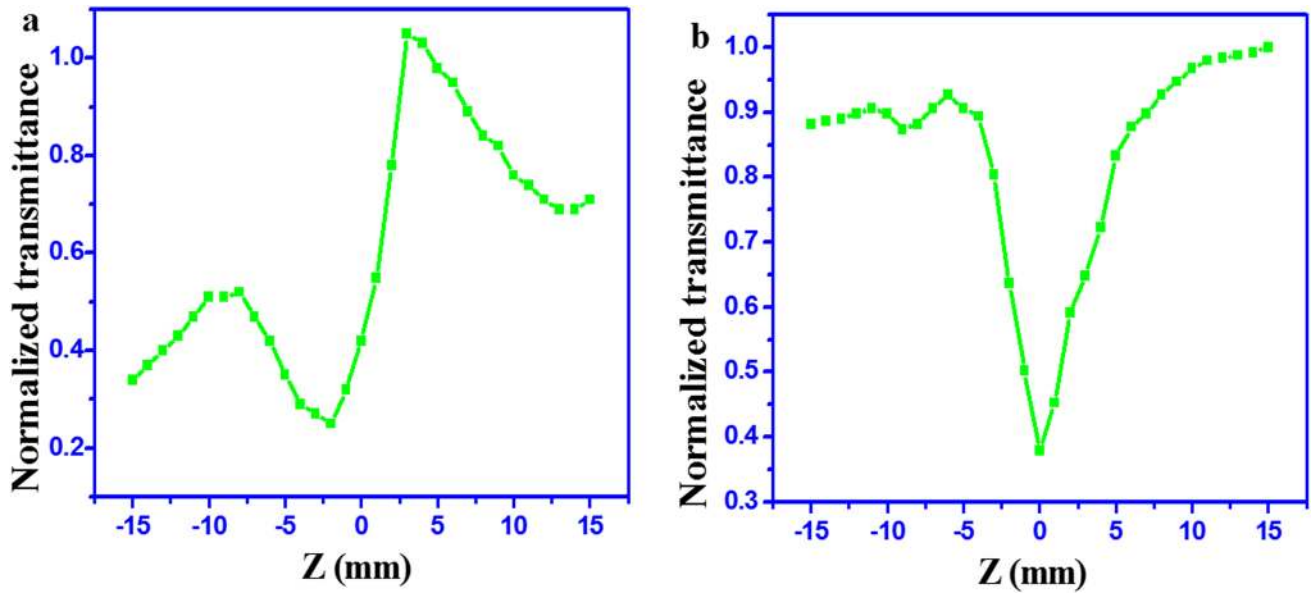
Fig. 7 **a** Closed aperture spectrum of CYHPH. **b** Open aperture spectrum of CYHPH

Gaussian beam profile. In the open aperture curve the minimum gained transmittance value at the focus (Z=0) reveals that the absorption is reverse saturable in CYHPH crystal (i.e., increasing of absorption coefficient resulting in the transmittance decrease with the increase in the input intensity). On-axis phase shift ($\Delta\Phi$) can be calculated from the peak and valley transmittance using the following equation [35].

$$\Delta T_{P-V} = 0.406(1 - S)^{0.25}|\Delta\phi| \tag{4}$$

here, S is aperture linear transmittance and it can be obtained from the relation $S = 1 - \exp(-2r_a^2/\omega_a^2)$, where r_a is the radius of the aperture and ω_a is the beam radius at the aperture. Third order nonlinear refractive index was calculated using closed aperture data and is given by [36]

$$n_2 = \frac{\Delta\phi}{KI_oL_{eff}} \tag{5}$$

where L_{eff} is the effective thickness of the crystal which was calculated using the following relation $L_{eff} = \frac{1-\exp(-\alpha L)}{\alpha}$ and K is the wave number (K=2π/λ). I_o is the intensity of the laser beam, α and L is the linear absorption and thickness of the sample respectively. From the open aperture data nonlinear absorption coefficient (β) was determined using the formula,

$$\beta = \frac{2\sqrt{2}\Delta T}{I_0L_{eff}} \tag{6}$$

where ΔT is the valley value at the open aperture curve. The nonlinear refractive index and nonlinear absorption coefficient were obtained and the values are 3.4855×10^{11} cm^2 W^{-1}, and 1.5681×10^{-4} cm^2 W^{-1} respectively.

The third order nonlinear optical susceptibility was calculated using the expression,

$$\chi^{(3)} = [(R_e(\chi^{(3)}))^2 + (I_m(\chi^{(3)}))^2]^{1/2} \tag{7}$$

The real and imaginary part of third order susceptibility was obtained from the formula,

$$R_e(\chi^{(3)})esu = \frac{10^{-4}\varepsilon_0 c^2 n_0^2 n_2}{\pi}\text{cm}^2\text{ W}^{-1} \tag{8}$$

Table 3 Nonlinear optical parameters for the CYHPH crystal

Laser beam wavelength (λ)	632.8 nm
Lens focal length (f)	30 mm
Optical path length	85 cm
Beam radius of the aperture (ω_a)	3.3 mm
Aperture radius (r_a)	2 mm
Sample thickness (L)	0.56 mm
Effective thickness (L_{eff})	0.5599 mm
Linear transmittance (s)	0.5203
Linear refractive index (n_0)	1.359
Nonlinear refractive index (n_2)	3.4855×10^{11}cm^2 W^{-1}
Nonlinear absorption coefficient (β)	1.5681×10^{-4}cm W^{-1}
Third order nonlinear susceptibility (χ)	3.6412×10^{-8}esu

Table 4 Comparison of χ^3 with some organic crystals

S. No	Crystal	Third order optical susceptibility χ^3(esu)	Reference
1	UPN	2.83×10^{-12}	[38]
2	GUCN	2.05×10^{-8}	[39]
3	Schiff base and their metal complexes (1, 1.a, 1.b, 1.d)	1.08×10^{-13} 0.18×10^{-13} 1.52×10^{-13} 1.02×10^{-13}	[40]
4	CYHPH	3.641×10^{-8}	Present work

$$I_m\left(\chi^{(3)}\right)esu = \frac{10^{-2}\varepsilon_0 c^2 n_0^2 \lambda\beta}{4\pi^2}\,cm^2\,W^{-1} \qquad (9)$$

where n_o is the linear refractive index of the crystal. The third order nonlinear optical parameters of CYHPH crystal are tabulated in Table 3.

Third order nonlinear susceptibility of some organic crystals are compared and specified in Table 4. The large value of third order nonlinear susceptibility (χ^3) can be attributed to the electron density transfer between donor and acceptor, resulting in the strong polarization within the molecular structure. Hence the results suggest that the crystal is an effective candidate for third order NLO applications [37].

4 Conclusion

An organic nonlinear optical cyclohexylaminium hydrogen phthalate hemi hydrate single crystal (CYHPH) was grown by slow evaporation technique and bulk crystal of CYHPH was grown by slow cooling method. The harvested size is $19 \times 15 \times 10$ mm^3. The lattice parameters were obtained (a$=$11.662 Å, b$=$14.152 Å, c$=$16.932 Å, $\alpha=\beta=\gamma=90°$ and volume V$=$2794.8 Å^3) using single crystal XRD analysis. The sharp peaks of powder XRD pattern indicate the good crystallinity nature. The presences of functional group were confirmed by FT-IR analysis. The decomposition temperature of CYHPH was found at 263 °C through thermal studies. Cut off wavelength was found to be 307 nm and optical band gap (4.08 eV) was calculated using Tauc's plot. The dielectric studies, carried out as a function of frequency which clearly showed the decrease in dielectric constant and dielectric loss with respect to the increased frequency. Low dielectric loss tells about the quality of the crystal with less defects. The AC conductivity was increased with frequency and the activation energy values were calculated at 100 Hz, 1 KHz and 10 KHz (0.31, 0.141 and 0.142 eV respectively) and it is low for this crystal. The

Z scan technique gives the value of the nonlinear absorption coefficient (1.5681×10^{-4} cmW^{-1}), the nonlinear refractive index (3.4855×10^{11}cm^2 W^{-1}) and third order nonlinear optical susceptibility (3.6412×10^{-8}esu). It is clear that the crystal has positive nonlinear refractive index due to the self-focusing effect and reverse saturable absorption. The above studies conclude that the CYHPH crystal is suitable for third order nonlinear optical applications.

References

1. M. Sarr, A. Diasse-Sarr, L. Diop, L. Plasseraud, H. Cattey, Acta Crystallogr. E, **71**, 899–901, (2015)
2. M.T. Han, Acta Crystallogr. E, **68**, o1579 (2012)
3. B. Wei, Acta Crystallogr. E, **67**, o2185 (2011)
4. M. Souhassou, P.M. Schaber, R.H. Blessing, Acta Crystallogr. B **52**, 865–875 (1996)
5. A. Lemmerer, J. Chem. Crystallogr. **42**, 498–503 (2012)
6. S. Krishnan, C. Justin Raj, S. Dinakaran, R. Uthrakumar, R. Robert, S. Jerome Das, J. Phys. Chem. Solids **69**, 2883–2887 (2008)
7. D. Saravanan, G. Ramesh Kumar, S. Gokul Raj, S. Mohan, B. Sivakumar, Spectrochim. Acta Part A **150**, 712–720 (2015)
8. J.V. Manonmoni, G. Ramasamy, A.A. Prasad, S.P. Meenakshisundaram, M. Amutha, RSC Adv. **5**, 46282–46289 (2015)
9. S.R. Marder, Chem. Commun. **2**, 131–134 (2006)
10. S. Basu, Ind. Eng. Chem. Prod. Res. Dev. **23**, 183–186 (1984)
11. M. Radha Ramanan, R. Radhakrishnan, T. Dhanabal, M. Sivaraju, R. Ashokkumar, Optik **126**, 5600–5604 (2015)
12. C.K. Lakshmana Perumal, A. Arulchakkaravarthi, N.P. Rajesh, P. Santhana Raghavan, Y.C. Huang, M. Ichimura, P. Ramasamy, J. Cryst. Growth **240**, 212–217 (2002)
13. V.N. Yadav, C.H. Görbitz, Cryst. Eng. Commun. **15**, 7321 (2013)
14. B. An, B. Bai, F. Yang, Z. Naturforsch. B Chem. Sci. **67**, 85–88 (2012)
15. B.R. Bhogala, S. Basavoju, A. Nangia, Cryst. Growth Des. **5**, 1683–1686 (2005)
16. C.B. Aakeroy, K.R. Seddon, Chem. Soc. Rev. **22**, 397–407 (1993)
17. J. Muszalski, Acta Phys. Polonica A, **114**, 983–999 (2008)
18. K.E. Maly, T. Maris, J.D. Wuest, Cryst. Eng. Commun. **8**, 33–35 (2006)
19. D. Kong, A. Clearfield, Cryst. Growth Des. **5**, 1767–1773 (2005)
20. C.Y. Liu, V. Lynch, A.J. Bard, Chem. Mater. **9**, 943–949 (1997)
21. N. Sudharsana, B. Keerthana, R. Nagalakshmi, V. Krishnakumar, L. Guru Prasad, Mater. Chem. Phys. **134**, 736–746 (2012)
22. R. Jagan, K. Sivakumar, Acta Crystallogr. C **67**, o373–o377 (2011)
23. R.M. Jauhar, V. Viswanathan, P. Vivek, G. Vinitha, D. Velmurugan, P. Murugakoothan, RSC Adv. **6**, 57977–57985 (2016)
24. P. Sathya, M. anantharaja, N. Elavarasu, R. Gopalakrishnan, Bull. Mater. Sci. **38**, 1291–1299 (2015)
25. M. Suresh, S. Asath Bahadur, S. Athimoolam, J. Mol. Struct. **1112**, 71–80 (2016)

26. C. Yogambal, R. Ezhil Vizhi, D. Rajan Babu, Cryst. Res. Technol. **50**, 22–27 (2014)
27. S. Sagadevan, P. Murugasen, J. Cryst. Pro. Tech **4**, 99–110 (2014)
28. Y. Wang, S. Pan, X. Tian, Z. Zhou, G. Liu, J. Wang, D. Jia, Inorg. Chem. **48**, 7800–7804 (2009)
29. L. Baouab, A. Jouini, J. Solid State Chem. **141**, 343–351 (1998)
30. G. Taha, J. Amor, Open J. Inorg. Chem. **1**, 47–53 (2011)
31. A. Silambarasan, M. Krishna Kumar, A. Thirunavukkarasu, R. Mohan Kumar, P.R. Umarani, J. Cryst. Growth **420**, 11–16 (2015)
32. M.R. Anantharaman, Bull. Mater. Sci. **25**(7), 599–607 (2002)
33. G.V. Anuradha, Optik **127**, 4004–4006, (2016)
34. I.P. Bincy, R. Gopalakrishnan, J. Cryst. Growth **402**, 22–31 (2014)
35. S. Arockia Avila, S. Selvakumar, M. Francis, A. Leo Rajesh, J. Mater. Sci. **28**, 1051–1059 (2016)
36. B. Dhanalakshmi, S. Ponnusamy, C. Muthamizhchelvan, V. Subhashini, J. Cryst. Growth **426**, 103–109 (2015)
37. P. Nagapandiselvi, C. Baby, R. Gopalakrishnan, RSC Adv. **4**, 22350–22358 (2014)
38. S. Selvakumar, A. Leo Rajesh, J. Mater. Sci. **27**, 7509–7517 (2016)
39. M. Dhavamurthy, R. Raja, K.S.S. Babu, R. Mohan, Appl. Phys. A **122**, 1–9 (2016)
40. N. Ananthi, U. Balakrishnan, S. Velmathi, K.B. Manjunath, G. Umesh, Opt. Photonics J. **2**, 40–45 (2012)